Which accelerator photon beams are "clinic-like" for reference dosimetry purposes?

N. I. Kalach[a)] and D. W. O. Rogers[b)]
National Research Council of Canada, Ottawa K1A OR6, Canada

(Received 8 July 2002; accepted for publication 12 March 2003; published 16 June 2003)

Previous work has demonstrated that, for photon beam dosimetry, TPR^{20}_{10} is not an ideal beam quality specifier for all bremsstrahlung beams, especially for lightly filtered beams in some standards laboratories. This paper addresses the following questions: Is TPR^{20}_{10} an adequate beam quality specifier for all modern clinical therapy accelerators? When can nonclinical beams in standards laboratories be used to calibrate ion chambers or measure k_Q factors as a function of TPR^{20}_{10}? Based on detailed Monte Carlo simulations of Varian, Siemens, Elekta, and GE (Saturn) accelerators one can conclude that TPR^{20}_{10} is an adequate beam quality specifier for all these machines in the sense that for a given value of TPR^{20}_{10}, the value of stopping-power ratios is the same. It is shown that, for the heavily filtered beams used in standards laboratories, TPR^{20}_{10} is an adequate beam quality specifier. It is also demonstrated that, for a larger range of bremsstrahlung beams than previously, $\%dd(10)_x$ is a good beam quality specifier for all clinical beams as well as the lightly and heavily filtered beams in some standards laboratories. A criterion, based on the measured values of TPR^{20}_{10} and $\%dd(10)_x$ for the beam, is proposed for determining whether a nonclinical beam is well specified by TPR^{20}_{10}. Agreement between calculations for specific accelerators and measured beam quality specifiers is shown to be good, but agreement with published data for a variety of clinical accelerators is not as good. Possible reasons for the discrepancy are discussed.
[DOI: 10.1118/1.1573205]

I. INTRODUCTION

To use a modern radiation dosimetry protocol (e.g., the AAPM's TG-51 protocol for high energy electron and photon beams[1] or the AAPM's TG-61 protocol for x-ray beams[2]) it is essential to specify the quality of the beam in order to select the values to use for various parameters. An ideal beam quality specifier is one that is easy to measure and for which all parameters of interest are uniquely specified. For accelerator photon beams there are two widely used specifiers, $\%dd(10)_x$, which is used by the AAPM's TG-51 protocol, and TPR^{20}_{10}, which is used by the older AAPM TG-21 protocol[3] and the IAEA's old and new Codes of Practice.[4,5] As Andreo[6] has pointed out "TPR^{20}_{10} can be meaningless if the accelerator potential and the target and filter combinations used to derive stopping-power data are completely ignored" and earlier he stated[7] "...stopping-power ratios... used today in dosimetry protocols will not necessarily apply to such accelerators (i.e., those in standards labs), not even when the quality of the beam is specified in terms of TPR^{20}_{10}."

Given the general agreement that TPR^{20}_{10} does not uniquely specify beam quality for all bremsstrahlung beams, a significant issue is whether TPR^{20}_{10} is an accurate beam quality specifier for all clinical beams. Originally Andreo and Brahme[8] showed a unique relationship between TPR^{20}_{10} and stopping-power ratios based on Monte Carlo calculations for a set of quite crudely measured or calculated clinical spectra from accelerators of an earlier era. In order to increase the data set available for clinical dosimetry, they used a set of bremsstrahlung spectra that they calculated for combinations of tungsten target and lead filter thicknesses considered by them as typical for clinical machines. They chose a single target thickness of $r_0/3$, where r_0 is the CSDA range at the energy of electrons incident on the tungsten target, and additional lead filtration ranging in thickness from 1 to 6 cm for the energy range 2–50 MV. They obtained very tight agreement between the $(\overline{L}/\rho)^{\mathrm{water}}_{\mathrm{air}}$ vs TPR^{20}_{10} curves for Mohan and other published spectra and for their Pb filtered "clinic-like" spectral data sets.[8]

Although the Mohan *et al.*[9] spectra used by Andreo and Brahme have been shown to still be representative of modern accelerators,[10] the physical parameters of modern clinical accelerators may differ substantially from the measured spectra available to Andreo and Brahme (a 2 MeV van de Graaff, 6 MV Mullard and 6 MV Vickers, betatrons, etc.) and certainly do not match the Andreo and Brahme calculated "clinic-like" spectra very closely. For a recent study of nine accelerator beams from the three major manufacturers of modern machines (Varian, Siemens, and Elekta), Sheikh-Bagheri and Rogers have found[10,11] that a typical modern clinical accelerator target is made of tungsten on a copper base, or gold, or of pure copper, with thicknesses much thicker than $r_0/3$ at the relevant electron energies for those materials (for example, some typical combinations are $0.7r_0$ tungsten with $0.3r_0$ copper, $0.2r_0$ tungsten with $0.7r_0$ copper, $0.7r_0$ copper, etc.). The typical flattening filters are made of a wide variety of materials, from aluminum to tungsten. They have very complicated shapes or combinations of shapes which are partially inserted within the primary collimator. Their thicknesses range from approximately 2 cm of copper to the 12 cm combined thickness of aluminum and stainless steel where "thickness" is evaluated as the distance from the apex of a quasiconical structure to its bottom. Those thicknesses are not directly comparable to the thicknesses of flat lead filtration used by Brahme and Andreo.[8] It is also known that some clinical accelerators, such as the racetrack microtron machines, use thin targets and in common with the new tomotherapy units, do not have a flattening filter.

One of the purposes of the present study is to ask, is TPR_{10}^{20} an adequate beam quality specifier for the range of modern clinical beams? We show in the following that it is, consistent with the much earlier results of Andreo and Brahme[8] (except for the swept beams of the racetrack microtron).

However, this still leaves one significant problem for protocols which allow the use of measured k_Q factors and use TPR_{10}^{20} as a beam quality specifier. Many standards laboratories have nonclinical accelerators (e.g., those of Canada, Belgium, Australia, and the United Kingdom) and even those that do have clinical machines have frequently modified them, or they are ''unusual'' in some other sense. So the question arises, when can we say that a calibration beam is ''clinic-like.'' That is, when can measured calibrations of ion chambers as a function of TPR_{10}^{20} be used with confidence in clinical beams (by which we mean all currently used beams which are heavily filtered)?

Kosunen and Rogers[12] noted that stopping-power ratios and TPR_{10}^{20} values for aluminum thick target spectra filtered by 14 cm of aluminum are very close to the curve for ''clinical spectra'' that they calculated and suggested that this confirms the approach of the UK's National Physical Laboratory (NPL) of using thick aluminum filters to make their thick target spectra more ''clinic-like.'' At that time, Andreo argued that, since the targets and flattening filters used at NPL are much thicker than those used in clinical accelerators, they cannot be considered equivalent to those used in clinical practice[13] although these are the beams currently used by the NPL as ''clinic-like'' and accepted as such by the TRS-398 Code of Practice.[5]

Since the new IAEA Code of Practice offers no quantitative criterion for what constitutes a clinical beam, it would be possible for a user following this Code of Practice to send an NE2611 ion chamber to both NPL and NRC and request a measured k_Q value for a beam with a TPR_{10}^{20} value of 0.792. Based on published values of measured k_Q values from each laboratory,[14] the factors received would differ by about 1.1%. The IAEA TRS-398 Code of Practice provides no criterion for knowing which was correct, or whether either was applicable in a clinical beam.

The goal of the current work is to provide just such a criterion. The brute force approach is to do a full Monte Carlo simulation of each calibration beam and determine if it is ''clinic-like'' in the sense that its calculated stopping-power ratio as a function of TPR_{10}^{20} falls on the standard curve for clinical beams. This approach is used here for beams at NRC and NPL. This requires special expertise. We also propose a criterion which is much simpler to apply. The ''clinic-like'' status of a calibration beam is determined based on the measured values of TPR_{10}^{20} and $\%dd(10)_x$. By using such a criterion to establish the ''clinic-like'' nature of the calibration beam, the use of TPR_{10}^{20} as a beam quality specifier when using measured k_Q values can be rigorously defended for standard clinical machines. Unfortunately, as will be discussed in the following, the measured data concerning this criterion for clinical accelerators is not in good agreement with the calculated results although agreement for beams in standards laboratories is acceptable.

Another issue is how to calibrate those beams from machines that do not fall on this ''clinic-like'' curve, namely the Racetrack microtrons and possibly any new machines which have lightly filtered beams. If using TPR_{10}^{20} as a beam quality specifier, these machines require special treatment, whereas if one uses $\%dd(10)_x$, they are treated like all other beams [although strictly speaking this has only been established for the Racetrack microtrons, the wide range of beams for which $\%dd(10)_x$ is shown to work strongly suggests it will work for all beams from possible new clinical accelerator types].

II. CALCULATIONAL DETAILS

The quantities that must be calculated for this study are: $(\overline{L}/\rho)_{\rm air}^{\rm water}$, the Spencer-Attix restricted mass collision stopping power ratio, water to air, at 10 cm depth in a water phantom irradiated by a $10\times10\ \mathrm{cm}^2$ beam; $\%dd(10)_x$, the photon component of the percentage depth-dose at 10 cm depth in a $10\times10\ \mathrm{cm}^2$ beam at a source–surface distance (SSD) of 100 cm; and TPR_{10}^{20}, the ratio of dose or ionization measurements at 10 and 20 cm depth at a fixed source–detector distance (SDD) of about 100 cm for a $10\times10\ \mathrm{cm}^2$ beam at the point of measurement. All calculations are done using the EGS4/PRESTA system for Monte Carlo simulations.[15,16] The BEAM user-code[17] is used to calculate various spectra as well as all the beam quality specifiers.

II. A. Photon beam spectra

The calculations of stopping-power ratios and beam quality specifiers described in the following require detailed photon spectra for a wide number of accelerator beams. A number of photon spectra measured or calculated elsewhere have been used. They are described briefly in the Appendix and many were used previously by Kosumen and Rogers.[12] The other spectra have been calculated in the present work (for the NRC standard beams and the NRC soft and hard filtered beams) using full simulations of the NRC linac with varying incident electron energies and flattening filter thicknesses. Details of the new simulations are described in the following.

II. A. 1. Calculation of photon spectra using the BEAM system

NRC 10, 20, and 30 MV photon beams. Sheikh-Bagheri *et al.*[18] did detailed BEAM Monte Carlo simulations of the 10 and 20 MV photon beams of the NRC linac, which have been used for standards work at NRC.

The NRC standard 10 and 20 MV photon spectra are calculated using the BEAM input files of Sheikh-Bagheri *et al.*[18] In addition, those files are modified as follows for a simulation of the 30 MV NRC standard photon beam. The target for the 30 MV beam is a fully stopping aluminum block, 6.0 cm thick. The electron beam energy of the NRC linac is

TABLE I. Geometry characteristics of the NRC soft and hard beams used in the Monte Carlo simulations.

Beam label	Target thickness (cm Al)	Sweep angle (°)	Hardener thickness (cm Al)
NRC soft 10 MV	2.5	4.2	0
NRC soft 20 MV	4.5	4.2	0
NRC soft 25 MV	5.2	3.4	0
NRC soft 30 MV	6.0	2.8	0
NRC hard 20 MV	4.5	4.2	10
NRC hard 25 MV	5.2	3.4	15
NRC hard 30 MV	6.0	2.8	15

known to ±1% and the electron beam energy distribution in the 30 MV BEAM simulation was taken as a Gaussian distribution with a full width at half maximum (FWHM) equal to 1% of the nominal energy. The electron beam incident on the target is scanned on the surface of a cone with a half angle of 2.8° to obtain field flatness. The apex of the cone is positioned on the front surface of the target. Due to imperfections in the scanning coil the beam wobbles inside a circle of 0.2 cm at the front surface of the target. The intensity distribution of the 30 MV electron beam was taken as a Gaussian with FWHM of 0.326 cm. [from Carl Ross (private communication)]. For benchmarking purposes, values of TPR_{10}^{20} for all three beams have been calculated[19] and compared to those measured at NRC[14] and agree within 0.004. The spectra used in the present calculations are for 100 cm^2 fields at an SSD of 100 cm.

NRC hard and soft beams. In the early 1990s, Ross *et al.* did measurements in a series of beams generated at 10, 20, 25, and 30 MeV incident electron energy using a swept beam and a fully stopping target with or without extra aluminum filters.[20] The soft and hard photon beams ranging from 10 to 30 MV generated from the NRC linac have been modeled by Yang *et al.*[19] using the BEAM code. The hard filtration refers to an additional 10–15 cm of aluminum located after the aluminum target. The Monte Carlo simulated photon beams with hard and soft filtration have been validated by comparing tissue-phantom ratios calculated by the BEAM code to those measured by Ross *et al.*[20] and values agreed within the experimental uncertainty of 0.5%.[19]

The spectra of the NRC hard and soft beams have been obtained using the BEAM input files from Yang *et al.*,[19] modified to define a field size of $10\times10\ \mathrm{cm}^2$ at 100 cm SSD ($10\times10\ \mathrm{cm}^2$ at 120 cm SDD in the original paper) and to include a slab of air below the collimator. Simulations of these NRC hard and soft beams generated from the NRC linac included the titanium exit window, aluminum target, a square collimator and, in the case of the hardened beam, additional aluminum filtration below the target. Geometric characteristics of the beams used in the simulations are summarized in Table I. Electron swept beams were simulated using the BEAM source option where the incident beam is a monoenergetic parallel circular beam of radius 0.26 cm, the axis of which sweeps the surface of an imaginary cone with a sweep angle as in Table I.

II. B. Stopping-power ratios

The stopping-power ratios are calculated using the EGS4 user-code SPRRZ,[12,21] which calculates Spencer-Attix stopping-power ratios in a cylindrical geometry starting from an input photon spectrum. SPRRZ uses an on-the-fly scoring technique described in detail in the manual for SPRRZnrc, a new version of the same code which works with the EGSnrc system.[22] All calculations are done using electron stopping powers from ICRU Report 37.[23]

In all cases the reported water to air stopping-power ratios are at 10 cm depth and averaged over a 1-cm-thick disk of radius 2 cm. The incident source is a point 100 cm away from the phantom surface and collimated to 100 cm^2. The statistical uncertainties were typically 0.01% based on 10^7 histories. Stopping-power ratio values in this work agree within 0.1% with previous values, although for an unknown reason there is a tendency for the current values to be about 0.1% higher than found previously.[12,21]

II. C. TPR_{10}^{20}

Values of TPR_{10}^{20} are determined by calculating the depth-dose curve, $D(z)$, on the central axis in a normally incident parallel beam of photons with the specified energy spectrum. The beam is $10\times10\ \mathrm{cm}^2$ and the scoring region 5 mm in radius. The value of TPR_{10}^{20} was originally extracted by fitting the region from 10 to 22 cm to $D(z)=D_0e^{-\mu z}$, where z is the depth and setting $\mathrm{TPR}_{10}^{20}=D(20)/D(10)=e^{-10\mu}$. However, this value is systematically lower (by up to 0.5%) than the simple two point value based on the ratio of doses at depths at 20 and 10 cm and so the latter values are used. The statistical uncertainty is reduced to less than 0.1% by using 2 billion initial histories in all cases.

II. D. $\%dd(10)_x$

Values of $\%dd(10)_x$ are calculated using the BEAM code with a point source spectrum at 100 cm incident on a square $10\times10\ \mathrm{cm}^2$ field. The dose is scored on the central axis in disks of radius 1.5 or 2 cm and thicknesses of 0.3 cm for the first 7.5 cm and 1 cm thereafter. The phantom is 40 cm thick and 28.2 cm in radius. Typically 1 to 2 billion initial photon histories are used in order to get the statistical uncertainties below 0.1% for the doses scored in each bin.

II. E. Mean energies

To elucidate the difference between TPR_{10}^{20} and $\%dd(10)_x$ as beam quality specifiers, we do some calculations with the FLURZnrc user code.[22] Photon spectra are incident from a point source at 100 cm SSD and the code calculates the mean energy as a function of depth on the central axis (radius<2 cm) of a water phantom of 30 cm diameter and 30 cm depth. These are the only calculations in this study done with EGSnrc[24,25] instead of EGS4. The differences between the codes in this situation are expected to be negligible.

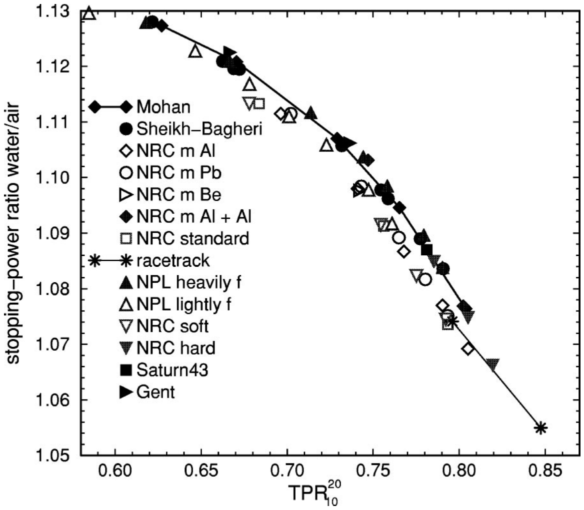

FIG. 1. Spencer-Attix water to air stopping-power ratios calculated with SPRRZ (based on the ICRU 37 stopping powers) vs TPR^{20}_{10} (calculated with the BEAM code for a parallel beam incident on a water phantom) for 14 sets of beams. All heavily filtered beams, i.e., clinical and "clinic-like," are shown as closed symbols. Beams referred to as "NRC m Al," etc., are measured (Ref. 38) thick target beams where "Al," etc., refers to the material of the target, and "+Al" means additional aluminum filtration.

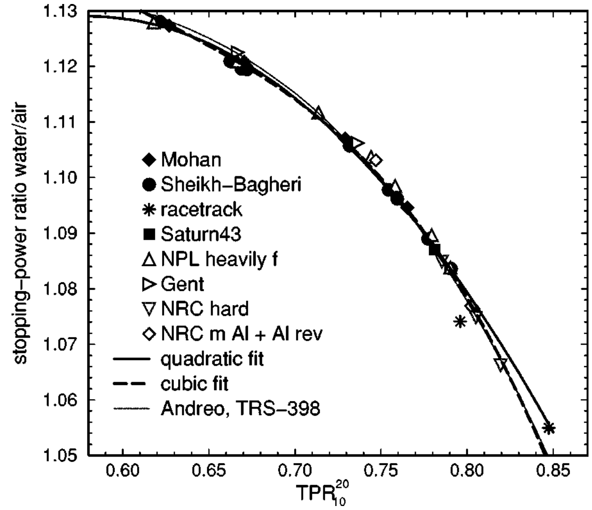

FIG. 2. Same as Fig. 1 but only for clinical beams (closed symbols) and the heavily filtered beams at several standards laboratories (NRC, NPL, Gent, open symbols). In addition the short-dashed line is a quadratic fit and the solid line a cubic fit [Eq. (1)] to just the clinical beams (excluding the racetrack beams). For comparison, the cubic fit used in the TRS-398 protocol is shown as the long dashed line (Ref. 5).

III. RESULTS

III. A. Stopping-power ratios as a function of TPR^{20}_{10}

Figure 1 presents our calculated values of stopping-power ratios as a function of TPR^{20}_{10}. These data are very similar to those published by Kosunen and Rogers[12] but include many more bremsstrahlung beams.

The most important result in Fig. 1 is that the ten new results for clinical beams (viz. the Saturn43 beam modeled by Menghi[26] and the nine beams from currently used Varian, Elekta, and Siemens clinical accelerators modeled by Sheikh-Bagheri and Rogers[10]) all lie on the same curve as the five beams modeled by Mohan *et al.*[9] With the exception of the clinical beams from the MM50 racetrack microtron, all clinical beams lie on a single curve. This confirms the earlier results of Andreo and Brahme[8] which were based on far cruder estimates of clinical accelerator spectra, and spectra measured for another generation of clinical machines.

A second important observation is that all heavily filtered beams (closed symbols) fall on this same curve. Thus, for example, the heavily filtered beams at NRC and the NPL fall on this curve as does the beam used by the Belgian standards lab. This is despite the fact that these beams in calibration labs sometimes bear little resemblance to clinical beams in how they are generated (different target and filter materials compared to most clinical beams).

Another interesting observation is that with the larger number of spectra used here, it becomes evident that all of the lightly filtered nonclinical beams also appear to fall onto a second curve with lower values of stopping-power ratio for a given value of TPR^{20}_{10}. For values of TPR^{20}_{10} near 0.8, the difference can be up to 0.7% but as little as 0.2% for TPR^{20}_{10} values near 0.65. It is the existence of this second family of data points which caused Kosunen and Rogers to conclude that TPR^{20}_{10} is not a universal beam quality specifier.[12]

Figure 2 presents the same data for just the clinical and heavily filtered beams along with cubic and quadratic fits to the clinical beam data only. Over the TPR^{20}_{10} range being fit (0.622 to 0.804) the fits are almost indistinguishable although they diverge slightly outside this range. On account of the improved agreement with the highest energy NRC hard beam, we chose to use the cubic fit which, for $TPR^{20}_{10}>0.62$, is given by

$$\left(\frac{\overline{L}}{\rho}\right)^{\text{water}}_{\text{air}} = 2.131 - 4.533(TPR^{20}_{10}) + 7.052(TPR^{20}_{10})^2 - 3.788(TPR^{20}_{10})^3. \tag{1}$$

The thin-line curve in Fig. 2 was calculated by Andreo[7] and is used in the IAEA TRS-398 Code of Practice.[5] For low-energy beams of a given value of TPR^{20}_{10}, the Andreo stopping-power ratios are up to 0.2% higher than the present cubic fit. For example, for a beam with a TPR^{20}_{10} value of 0.66, the present fit gives a stopping-power ratio of 1.1220 and the fit from Andreo gives 1.1235. Conversely, for a stopping-power ratio of 1.120, the Andreo fit implies a TPR^{20}_{10} value of 0.678 and the present cubic fit, only 0.669. The agreement is excellent for TPR^{20}_{10} values above 0.74. These differences are not important in view of the overall uncertainty in the stopping-power ratio, but they are not completely understood. Andreo presents[7] tabulated values for monoenergetic beams and, for example, for a 3 MeV beam our calculated stopping-power ratio agrees to four significant figures (1.117). Our calculated TPR^{20}_{10} value of 0.7233 is only 0.1% less than his values of 0.724 and our value at 2 MeV are even closer to each other.

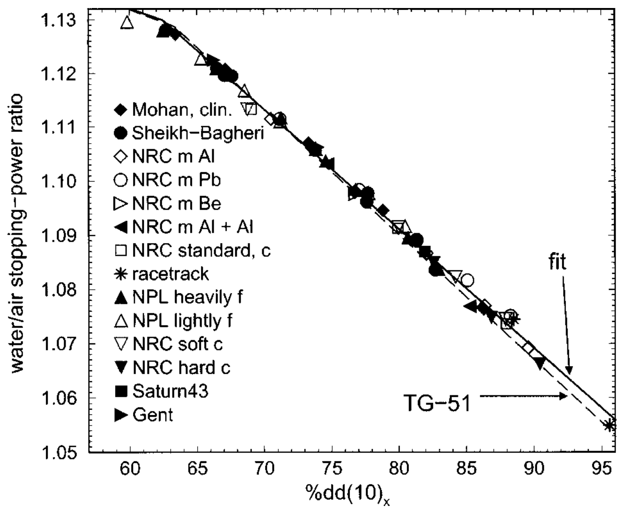

FIG. 3. Stopping-power ratios as in Fig. 1 except plotted vs $\%\mathrm{dd}(10)_x$. The fit, shown as the solid line, is given by Eq. (2) with a rms deviation 0.0012 and a maximum deviation 0.0027. The long dashed line is the fit (Ref. 21) which is used in TG-51—Ref. 1 (note that there are two straight lines with the break at 63.4%).

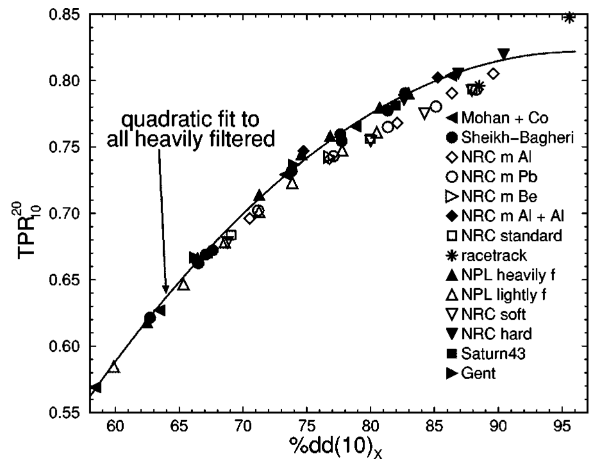

FIG. 4. Calculated values of TPR^{20}_{10} vs $\%\mathrm{dd}(10)_x$ for the same 14 sets of spectra as in Figs. 1 and 3. The line is a quadratic fit to all the heavily filtered beams which are shown as closed symbols. The fit to a third-order polynomial is given by Eq. (3) with an rms deviation 0.0037 and a maximum deviation 0.007 in TPR^{20}_{10}.

III. B. Stopping-power ratios as a function of $\%\mathrm{dd}(10)_x$

Figure 3 presents the same stopping-power ratio data as in Fig. 2 except now plotted as a function of the beam quality specifier $\%\mathrm{dd}(10)_x$. As found previously by Kosunen and Rogers,[12] the stopping-power ratios for all of these spectra fall on a single curve. The data with $\%\mathrm{dd}(10)_x$ greater than 62.46% fit a straight line given by

$$\left(\frac{\overline{L}}{\rho}\right)^{\mathrm{water}}_{\mathrm{air}} = 1.2676 - 0.002\,204(\%\mathrm{dd}(10)_x), \tag{2}$$

where the lightly filtered 4 MV beam from the NPL ($\%\mathrm{dd}(10)_x = 59.9\%$) is excluded from the fit. The rms deviation is 0.0012 and the maximum deviation is 0.0027. The figure also presents the curve which is used in the calculations of k_Q in the AAPM's TG-51 protocol.[21] Note that the TG-51 values are not a single straight line but two straight lines with the break at $\%\mathrm{dd}(10)_x = 63.4\%$ and for the present calculations this break is made at 62.46%.

The present data are in good agreement with the previous calculations and confirm the previous conclusion that $\%\mathrm{dd}(10)_x$ is a good beam quality specifier in the sense that it uniquely specifies the clinical, ''clinic-like'' and nonclinical beams.

III. C. Relationship between TPR^{20}_{10} and $\%\mathrm{dd}(10)_x$

Figure 4 plots the calculated values of TPR^{20}_{10} as a function of $\%\mathrm{dd}(10)_x$. Figure 4 includes all of the calculated results shown in Figs. 2 and 3. The solid line is a quadratic fit to the all of the heavily filtered data, namely:

$$\mathrm{TPR}^{20}_{10} = -0.8228 + 0.0342(\%\mathrm{dd}(10)_x) - 0.000\,1776 \times (\%\mathrm{dd}(10)_x)^2 \tag{3}$$

The rms deviation of the data about the fit is 0.0034 and the maximum deviation in TPR^{20}_{10} values is 0.007. A cubic fit to the same data and fits to the data for just the clinical beams are practically indistinguishable. The fit can also be performed in the other direction giving

$$\%\mathrm{dd}(10)_x = -430.62 + 2181.9(\mathrm{TPR}^{20}_{10}) - 3318.3(\mathrm{TPR}^{20}_{10})^2 + 1746.5(\mathrm{TPR}^{20}_{10})^3. \tag{4}$$

In this case, a cubic function is essential to get a good fit. The rms deviation is 0.46 and the maximum deviation in values of $\%\mathrm{dd}(10)_x$ is 0.9%.

Figure 4 shows two families of beams, corresponding to the two families of beams in Fig. 1, one the clinical and ''clinic-like'' beams, the others the lightly filtered, ''other'' beams.

This tight grouping of all the clinical and heavily filtered beams suggests a criterion for establishing if a beam is ''clinic-like'' in the sense that its stopping-power ratio at 10 cm depth is well specified by the TPR^{20}_{10} beam quality specifier. One measures the values of TPR^{20}_{10} and $\%\mathrm{dd}(10)_x$ and sees if they lie on the curve within some acceptable tolerance. If so, the beam is ''clinic-like,'' and if not, then TPR^{20}_{10} does not specify the quality of the beam and one must use $\%\mathrm{dd}(10)_x$. Unfortunately, the sensitivity of this criterion is not as great as one might like. For example, Fig. 1 shows that the standard 10 MV beam at NRC is not ''clinic-like'' and yet its calculated value of TPR^{20}_{10} is only 0.006 below the fitted line in Fig. 4. The TPR^{20}_{10} value for NRC's 30 MV beam is 0.016 below the curve and thus this beam clearly is not ''clinic-like'' on this basis, as well as based on the results in Fig. 1.

Note that this criterion is only useful for standards labs to establish whether their beams are ''clinic-like'' or not, but is not needed for those beams reported here since Fig. 1 demonstrates directly whether they are ''clinic-like'' or not. This criterion would also be relevant for any new design of accel-

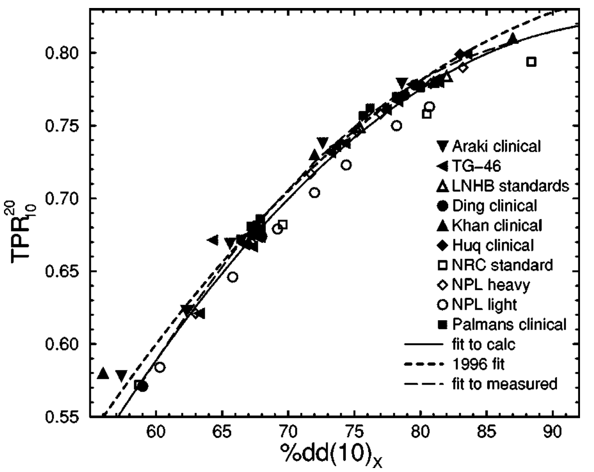

FIG. 5. Measured vs fitted values of TPR^{20}_{10} vs %dd(10)$_x$. The solid line is the fit to the calculated heavily filtered beams shown in Fig. 4 [Eq. (3)]. Closed symbols are published measured data for clinical beams (Refs. 27–31) and the data from the TG-46 compendium (Ref. 34). Open symbols are measured data from standards laboratories (Refs. 14, 32, 33). Note the NRC data point for ^{60}Co uses BJR25's value for %dd(10)$_x$. The long dashed line is a quadratic fit [Eq. (5)] to the measured data for clinical beams (excluding the two ^{60}Co results with lowest values of %dd(10)$_x$). Also shown for comparison is an early crude fit (short dashed line) to similar data by Kosunen and Rogers for the Mohan spectra and the 50 MV racetrack beam (Ref. 35). Note that the data of Khan was given to only two significant figures (Ref. 31).

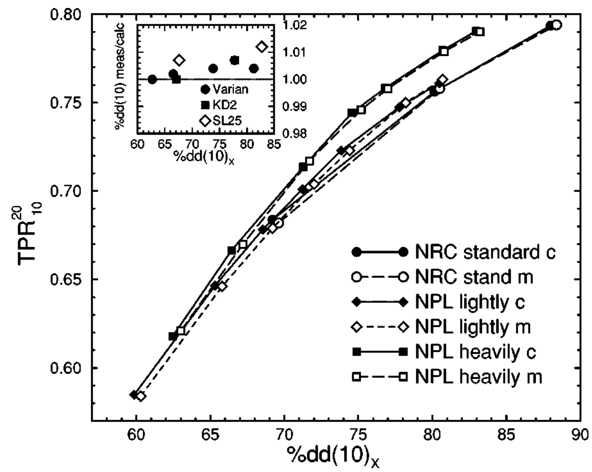

FIG. 6. Comparison of measured and calculated values of TPR^{20}_{10} vs %dd(10)$_x$. In the main panel, open symbols and dashed lines represent measured data while closed symbols and solid lines are the calculated results. The inset shows the ratio of %dd(10) from the measured data set used by Sheikh-Bagheri to the value of %dd(10)$_x$ calculated here and corrected using Sheikh-Bagheri's calculated electron contamination for each beam (Ref. 10).

erator which is dissimilar to current machines (e.g., the new tomotherapy machines, except that they do not have 10 $\times$10 cm^2 fields).

Figure 5 presents the same fit to the heavily filtered data in Fig. 4 along with a variety of individually measured data taken from various papers[14,27–33] and data based on the AAPM's TG-46 report which included averaged %dd curves and TPR^{20}_{10} data tables for a large variety of accelerator beams[34] [%dd(10)$_x$ is deduced from %dd(10) using the general formula given in the TG-51 protocol[1]]. The NPL data are based on the measured values from NPL but the measured values of %dd(10)$_x$ had to be corrected to account for electron contamination and different field sizes and SSD.[32]

The short dashed line in Fig. 5 shows a crude fit which was needed in the calculation[35] of k_Q factors for the TG-51 protocol.[1] This fit was based on the calculated data of Kosunen and Rogers for the Mohan series of spectra and the 50 MV racetrack spectrum.[12] These data needed to be corrected[21] and the present data have higher statistical precision as well as many more data points in the fit. Also, the 50 MV data point is no longer included in the fit since it is not "clinic-like" as defined here. Nonetheless, the previous fit appears to agree somewhat better with the measured data than the current fit to the calculated data (solid line, Fig. 5) although the measured data are scattered.

The long dashed line in Fig. 5 is a quadratic fit to the measured clinical data in this figure (excluding the two ^{60}Co data points with the lower %dd(10)$_x$ values). The fit is given by

$$TPR^{20}_{10} = -0.9305 + 0.037\,24(\%dd(10)_x) - 0.000\,198\,3(\%dd(10)_x)^2. \quad (5)$$

The rms deviation of the data about the fit is 0.007 and the maximum deviation in TPR^{20}_{10} is 0.011 [ignoring the one outlier with %dd(10)$_x$=64.3% from the TG-46 data for a Clinac-6X].

Many of the measured data for clinical beams are above the present fit to the calculated data. This is not understood since, for those cases in which there are direct comparisons between measured and the present (average spectrum) calculated values for beams at NRC and NPL, the agreement tends to be within 1% or often much better. Figure 6 presents a comparison of these measured and calculated data for standards labs beams. It can be seen that although the calculated and measured values of TPR^{20}_{10} and %dd(10)$_x$ may disagree with the measurements by up to 1%, they do so in a manner which leaves the TPR^{20}_{10} vs %dd(10)$_x$ curve unaffected (i.e., the dashed and solid line for a given set of data are very similar). If anything, the measured curves are below the calculated curves, which is the reverse of the case for the clinical beams. One would expect that the differences seen between the measured and calculated values of %dd(10) for the clinical machines, which are of the same order as the differences seen with the standards labs machines (see inset, Fig. 6), would also not affect the overall curve. Nonetheless, for example, the measured clinical data of Palmans *et al.*[30] can be thought of as having TPR^{20}_{10} values which are 1.5% above the curve fitted to the calculated data, or the %dd(10)$_x$ values are 2% (2.7% relative) lower than those calculated. These are close to worst cases, and, in particular, it is worth noting that with one exception, the averaged data from the TG-46 report are in good agreement with the calculated values.

In an effort to understand these discrepancies, we calculate, for the Varian 6 and 18 MV beams, the TPR_{10}^{20} values using point source beams at SSD=80 and SSD=90 cm, with field sizes of $10\times10\ \mathrm{cm}^2$ at the detector position (SSD=100 cm). The results for this more realistic calculation agree (within 0.1% on average) with the values calculated with a parallel beam, as done in the rest of the present calculations and as done in previous calculations of TPR_{10}^{20}. However, if rather than using spectra, we do the same calculations for a full phase space file, we find that the TPR_{10}^{20} values calculated this way are 0.8% and 0.5% higher than when using a photon spectrum as source (and for the 18 MV beam, are in good agreement with the measured value of TPR_{10}^{20} for the 18 MV Varian beam at the Fraser Valley Cancer Clinic). At the same time, the values of $\%dd(10)_x$ calculated with the full phase space simulation agreed within statistics (which varied from 0.1% to 0.3%), with the point source calculations using a spectrum. These results together imply that the full phase space calculation of TPR_{10}^{20} would move the calculated values about 1/2 of the way toward the fit to the measured data in Fig. 5. This needs further investigation but is a major undertaking (a typical calculation takes 200 h on a 1.8 GHz CPU). Furthermore we do not have sufficient information to redo all the calculations this way. However, in the process of this project we have calculated $\%dd(10)_x$ for 26 beams using a full phase space calculation and if we compare these results to those calculated using the point source and average spectrum model, we find the average difference is 0.04 with a sample deviation of 0.29. This implies that there is nothing wrong with the simple model for calculating $\%dd(10)_x$, although the rather large sample deviation indicates that the full phase space calculations have not been done with as much statistical precision nor with such tightly controlled parameters (e.g., variation in size of scoring regions, etc). The measured values may have considerable uncertainty as well, but unless there is a systematic error in most of the measurements (which seems unlikely), this cannot explain the observed difference.

Figure 5 does show that the measured values for the nonclinical lightly filtered beams at the NPL and NRC are clearly below the fitted line, thereby demonstrating that calibrations cannot be done in these beams in terms of TPR_{10}^{20}. This is consistent with the direct results in Fig. 1.

IV. MEAN ENERGIES IN THE PHANTOM AND BEAM QUALITY SPECIFIERS

In a preliminary effort to understand why $\%dd(10)_x$ and TPR_{10}^{20} specify beam qualities in different manners, we calculate the mean electron and photon energies as a function of depth on the central axis of a water phantom irradiated by a $100\ \mathrm{cm}^2$ beam from a point source at 100 cm SSD. Figure 7 shows the mean energies of the photons for four different beams (the 20 and 25 MV hard and soft beams at NRC) and Fig. 8 shows the mean energies of the electrons generated by these same photon beams. There are many interesting features of Figs. 7 and 8, but for the purposes here, it is important to note the ordering of the average energies on each graph compared to the corresponding beam quality specifiers. The average photon energy increases in the same order as the TPR_{10}^{20} values, but not the $\%dd(10)_x$ values. In contrast, the average electron energy increases in the same order as the $\%dd(10)_x$ values but not the TPR_{10}^{20} values. In other words, the $\%dd(10)_x$ values are more closely correlated with the electron spectra at a point in the phantom whereas the TPR_{10}^{20} values are more closely correlated with the photon spectra. Clearly, the electron spectra are correlated to the photon spectra as well, but the correspondence is not unique,

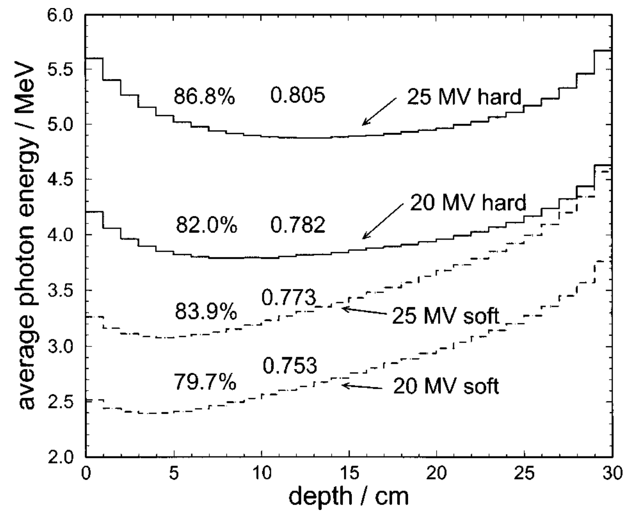

FIG. 7. Average photon energy on the central axis (0–2 cm radius) vs depth in a $100\ \mathrm{cm}^2$ beam for the NRC spectra shown. The values above each curve correspond to $\%dd(10)_x$ and TPR_{10}^{20} values for the beams. Note that the TPR_{10}^{20} values increase with increasing average energy of the beam whereas the $\%dd(10)_x$ values do not. Values are calculated using FLURZnrc (Ref. 22).

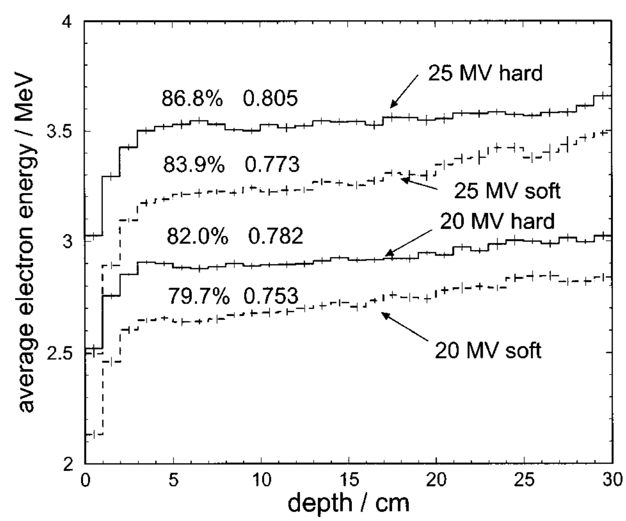

FIG. 8. Average electron energy on the central axis (0–2 cm radius) vs depth in a $100\ \mathrm{cm}^2$ beam for the NRC spectra shown. The values above each curve correspond to $\%dd(10)_x$ and TPR_{10}^{20} values for the beams. Note that the $\%dd(10)_x$ values increase with increasing average energy of the electrons whereas the TPR_{10}^{20} values do not, i.e., the order of the curves changes for photon and electron average energies. Values are calculated using FLURZnrc (Ref. 22).

as this rather extreme case points out. Since stopping-power ratios and other dosimetric quantities are more closely tied to the electron spectra at a given point, it should not be surprising that $\%dd(10)_x$ is a good beam quality specifier for a wider range of beam qualities.

V. SUMMARY AND CONCLUSIONS

The data presented in Figs. 1 and 2 demonstrate that TPR^{20}_{10} is an adequate beam quality specifier for the broad range of clinical accelerators currently available, except for the racetrack microtron which is only lightly filtered. This confirms the much earlier result of Andreo and Brahme,[8] which was based on calculations for spectra from an earlier generation of accelerators and some crude models of heavily filtered beams. The present results also demonstrate that all heavily filtered beams appear to lie on the same curve as the clinical spectra. Thus it is possible to use nonclinical beams to calibrate ion chambers in terms of TPR^{20}_{10} for use in clinical beams, as long as the beam has been established to be "clinic-like." Figures 1 and 2 explicitly demonstrate the "clinic-like" nature of the heavily filtered beams in the standards labs at NPL, NRC, and Gent. Figure 4 presents a criterion for establishing if a beam is "clinic-like" based on the measured values of TPR^{20}_{10} and $\%dd(10)_x$. This criterion is only relevant for standards labs. Unfortunately the measured data available in the literature for clinical beams are not in particularly good agreement with this criterion except for the averaged data presented in the TG-46 report[34] which scatters about the calculated line. Also the measurements made in standards labs are in excellent agreement with the calculated curves.

The equations linking TPR^{20}_{10} and $\%dd(10)_x$ for clinical beams [Eqs. (3) and (4)] are in principle a useful check for those implementing TG-51. After measuring $\%dd(10)_x$, they can verify that it is consistent with their previously measured value of TPR^{20}_{10}, although as mentioned, currently measured data in the literature suggest that the measured TPR^{20}_{10} values appear to be higher than predicted by Eq. (3).

Another application of Eq. (3) is to calculate the effective clinical TPR^{20}_{10} value for a given nonclinical beam. For example, the 30 MV standard beam at NRC has a measured TPR^{20}_{10} value of 0.794(1) and a measured $\%dd(10)_x$ value of 88.4(1)%. It is known not to be "clinic-like" so that when asked for a calibration in terms of TPR^{20}_{10}, the value of $N_{D,w}$ is wrong by about 1% when used in a clinical beam. Using Eq. (3) tells us that the effective clinical TPR^{20}_{10} value for that beam is 0.811. Equation (1) suggests that the expected $N_{D,w}$ value is 0.9% lower than if the TPR^{20}_{10} were taken at its face value of 0.794. Similarly, the effective TPR^{20}_{10} values for the 20 and 10 MV standard beams at NRC are 0.778 and 0.696, respectively, rather than the measured values of 0.758(1) and 0.682(1). Using these effective TPR^{20}_{10} values would imply agreement within 0.1% between the values of k_Q measured using the Canadian and French absorbed-dose standards, as opposed to the differences of up to 1% found using measured values of TPR^{20}_{10} but consistent with the excellent agreement found using $\%dd(10)_x$ as the beam quality specifier.[33]

This concern about whether a beam is "clinic-like" or not is only relevant when using TPR^{20}_{10} as a beam quality specifier. If beams are specified in terms of $\%dd(10)_x$, the issue of whether a beam is "clinic-like" or not is not relevant because $\%dd(10)_x$ specifies all real bremsstrahlung beams adequately, i.e., all beams investigated are "clinic-like" when using $\%dd(10)_x$.

ACKNOWLEDGMENTS

We thank Hugo Palmans of Gent University and Enrico Menghi, then of Bologna University, for sending us their BEAM code input files, Carl Ross of NRC for information about the 30 MV beam at NRC, Pedro Andreo of the Karolinska Institute for details on the stopping-power ratio curve used by the IAEA's TRS-398 and Chen-Shou Chui of MSKCC for information about the original Mohan *et al.* spectra. We thank Blake Walters and Michel Proulx of NRC for their continued support of the NRC computing system for Monte Carlo calculations.

APPENDIX: SOURCES OF SPECTRA USED

Many of the spectra described in this Appendix have been distributed as part of the EGS4/EGSnrc code systems for Monte Carlo transport.[15,25] The spectra are distributed in the ENSRC format which is read by a variety of EGS4 and EGSnrc user-codes[22] (e.g., DOSRZnrc, FLURZnrc, etc.). They are available via http://www.irs.inms.nrc.ca/inms/irs/EGSnrc/EGSnrc.html

1. Varian spectra calculated by Mohan *et al.*

Mohan *et al.*[9] used EGS3[36] to model various Varian accelerators viz. the Clinac-4 (4 MV), −6 (6 MV), −18 (10 MV), −20 (15 MV), and −2500 (24 MV). The spectra were verified by calculating tissue-maximum ratios in water.

These spectra have been used by a variety of authors over the years and have been distributed with the EGS4 system. During the present study it was found that the energy structure of the spectra referred to as the 15 and 10 MV Mohan spectra were different from the original spectra. These spectra have been re-digitalized from large scale plots supplied by Chen-Shou Chui and are used here. The implied changes in TPR^{20}_{10} are less than 0.003, and for stopping-power ratios, less than 0.05%.

2. Clinical accelerators

Sheikh-Bagheri and Rogers have modeled nine beams from clinical accelerators from the major manufacturers: Elekta SL25 6 and 25 MV beams; Siemens KD 6 and 18 MV beams; Varian Clinac-4 MV and Clinac 2100C/2300C 6, 10, 15, and 18 MV photon beam.[10,11,37] The simulations were benchmarked against measured depth-dose curves and in-air off-axis ratios. To obtain spectra for the present work, BEAM input files have been used with a set of incident electron beam parameters from Sheikh-Bagheri.[37] This set is slightly different from that presented in the final publications[10,11] but the differences have been shown to be unimportant to calculated photon spectra on the central axis in a 10×10 cm^2 field at 100 cm SSD.

Typical statistical uncertainties for the fluence per energy bin are 0.5% at the maxima of the spectra and 1%–1.5% elsewhere except for energy bins close to the maximum energy.

3. Racetrack Microtron calculated spectra

The spectra from the Memorial Sloan-Kettering Cancer Center's MM50 were modeled by Kosunen and Rogers using EGS4[12] and also used here. Note that different MM50 machines are configured differently and the models used were very simple.

4. NPL calculated spectra

Photon beams with nominal energy from 4 to 19 MV for the accelerator of the National Physical Laboratory (NPL) were modeled using BEAM.[32] Two sets of beams (''heavy'' and ''light'') differ by the amount of additional aluminum filtration added below the lower collimator and up to 4 cm of aluminum attached to the back of the target. Photon spectra have been calculated in the present work using the phase space files of Walters and Rogers,[32] collected at 118–120 cm SSD for a field size of 10×10 cm^2.

5. Thick target bremsstrahlung spectra measured at NRC

Bremsstrahlung spectra from thick targets of Al, Pb, and Be have been measured absolutely[38,39] in the sense of number of photons which emerge from the target into a given solid angle along the beam axis per electron incident on the target for electrons of 10, 15, 20, 25, and 30 MeV incident energy. The spectra have a 220 keV low-energy cutoff. The targets were cylinders with nominal thicknesses of 110% of the electron CSDA range. Typical uncertainties per energy bin were from 2% to 5% (systematic uncertainties in spectral measurements and uncertainties in the beam current are not included).

The pair of spectra referred to as ''NRC measured Al +Al'' have been obtained by Kosunen and Rogers[12] starting from the measured 10- and 20-MV-thick aluminum target spectra which were analytically filtered by an additional 14 cm of aluminum.

6. Saturn43 25 MV beam

Enrico Menghi has used BEAM to model the 25 MV beam of a Saturn43 accelerator and he has benchmarked his results against measured depth-dose curves.[26] He has provided his BEAM input files to us and the spectra for a 10×10 cm^2 field were generated at NRC using these inputs.

7. Gent 5 and 10 MV spectra

Gent University has an electron accelerator which they use for dosimetry standards work. As part of their standards work they have done detailed BEAM models of their two accelerator beams at 5 and 10 MV[40] and benchmarked their calculations against measured depth-dose curves. The accelerator has a Ta target and Pb flattening filter. The spectra presented here were calculated at NRC using BEAM and the input files developed by Palmans *et al.*[40] The spectra presented are averaged over a 10×10 cm^2 area in a nominal 12×12 field since the original values calculated by Palmans *et al.* were for these larger fields. Recent work[41] has provided data for nominal 10×10 cm^2 field sizes although these have not been used here.

[a]Present address: Fraser Valley Cancer Center, BCCA, 13750-96th Ave., Surrey, BC V3V 1Z2, Canada; electronic mail: nkalach@bccancer.bc.ca
[b]Electronic mail: dave@irs.phy.nrc.ca

[1] P. R. Almond, P. J. Biggs, B. M. Coursey, W. F. Hanson, M. S. Huq, R. Nath, and D. W. O. Rogers, ''AAPM's TG-51 Protocol for Clinical Reference Dosimetry of High-Energy Photon and Electron Beams,'' Med. Phys. **26**, 1847–1870 (1999).
[2] C.-M. Ma, C. W. Coffey, L. A. DeWerd, R. Nath, C. Liu, S. M. Seltzer, and J. Seuntjens, ''AAPM protocol for 40–300 kV x-ray beam dosimetry in radiotherapy and radiobiology,'' Med. Phys. **28**, 868–893 (2001).
[3] AAPM TG-21 ''A protocol for the determination of absorbed dose from high-energy photon and electron beams,'' Med. Phys. **10**, 741–771 (1983).
[4] IAEA, *Absorbed Dose Determination in Photon and Electron Beams: An International Code of Practice*, Technical Report Series Vol. 277 (IAEA, Vienna, 1987).
[5] IAEA, *Absorbed Dose Determination in External Beam Radiotherapy: An International Code of Practice for Dosimetry Based on Standards of Absorbed Dose to Water*, Technical Report Series Vol. 398 (IAEA, Vienna, 2001).
[6] P. Andreo, ''On the beam quality specification of high-energy photons for radiotherapy dosimetry,'' Med. Phys. **27**, 434–440 (2000).
[7] P. Andreo, ''Improved calculations of stopping-power ratios and their correlation with the quality of therapeutic photon beams,'' IAEA-SM-330/62 in *Proc. of Symp. on Meas. Assurance in Dosimetry* (IAEA, Vienna, 1994), pp. 335–359.
[8] P. Andreo and A. Brahme, ''Stopping-power data for high-energy photon beams,'' Phys. Med. Biol. **31**, 839–858 (1986).
[9] R. Mohan, C. Chui, and L. Lidofsky, ''Energy and angular distributions of photons from medical linear accelerators,'' Med. Phys. **12**, 592–597 (1985).
[10] D. Sheikh-Bagheri and D. W. O. Rogers, ''Calculation of nine megavoltage photon beam spectra using the BEAM Monte Carlo code,'' Med. Phys. **29**, 391–402 (2002).
[11] D. Sheikh-Bagheri and D. W. O. Rogers, ''Sensitivity of megavoltage photon beam Monte Carlo simulations to electron beam parameters,'' Med. Phys. **29**, 379–390 (2002).
[12] A. Kosunen and D. W. O. Rogers, ''Beam quality specification for photon beam dosimetry,'' Med. Phys. **20**, 1181–1188 (1993).
[13] P. Andreo, ''The status of high-energy photon and electron beam dosimetry five years after the implementation of the IAEA code of practice in the Nordic countries,'' Acta Oncol. **32**, 483–500 (1993).
[14] J. P. Seuntjens, C. K. Ross, K. R. Shortt, and D. W. O. Rogers, ''Absorbed-dose beam quality conversion factors for cylindrical chambers in high-energy photon beams,'' Med. Phys. **27**, 2763–2779 (2000).
[15] W. R. Nelson, H. Hirayama, and D. W. O. Rogers, ''The EGS4 Code System, Report SLAC-265,'' Stanford Linear Accelerator Center, Stanford, CA, 1985.
[16] A. F. Bielajew and D. W. O. Rogers, ''PRESTA: The Parameter Reduced Electron-Step Transport Algorithm for electron Monte Carlo transport,'' Nucl. Instrum. Methods Phys. Res. B **18**, 165–181 (1987).
[17] D. W. O. Rogers, B. A. Faddegon, G. X. Ding, C.-M. Ma, J. Wei, and T. R. Mackie, ''BEAM: A Monte Carlo code to simulate radiotherapy treatment units,'' Med. Phys. **22**, 503–524 (1995).
[18] D. Sheikh-Bagheri, D. W. O. Rogers, C. K. Ross, and J. P. Seuntjens, ''Comparison of measured and Monte Carlo calculated dose distributions from the NRC linac,'' Med. Phys. **27**, 2256–2266 (2000).
[19] C. L. Yang, D. W. O. Rogers, and J. P. Seuntjens, ''Calculation of photon beam quality specifiers,'' Proceedings of the 1998 COMP Annual Meet-

ing (Canadian Organization of Medical Physicists, Edmonton, Alberta), 1998, pp. 186–188.
[20] C. K. Ross, K. R. Shortt, D. W. O. Rogers, and F. Delaunay, *A Test of* TPR^{20}_{10} *as a Beam Quality Specifier for High-Energy Photon Beams, IAEA-SM-330/10*, in Proceedings of Symposium on Measurement Assurance in Dosimetry, (IAEA, Vienna, 1994), pp. 309–321.
[21] D. W. O. Rogers and C. L. Yang, ''Corrected relationship between $\%\mathrm{dd}(10)_x$ and stopping-power ratios,'' Med. Phys. **26**, 538–540 (1999).
[22] D. W. O. Rogers, I. Kawrakow, J. P. Seuntjens, and B. R. B. Walters, ''NRC User Codes for EGSnrc,'' Technical Report No. PIRS-702, National Research Council of Canada, Ottawa, Canada, 2000.
[23] ICRU, ''Stopping powers for electrons and positrons,'' ICRU Report No. 37, ICRU, Washington, DC, 1984.
[24] I. Kawrakow, ''Accurate condensed history Monte Carlo simulation of electron transport. I. EGSnrc, the new EGS4 version,'' Med. Phys. **27**, 485–498 (2000).
[25] I. Kawrakow and D. W. O. Rogers, ''The EGSnrc Code System: Monte Carlo simulation of electron and photon transport,'' Technical Report No. PIRS-701, National Research Council of Canada, Ottawa, Canada, 2000.
[26] E. Menghi, ''Simulazione di un acceleratore lineare radioterapico, mediante codice Monte Carlo BEAM,'' M.Sc. thesis, Bologna University, Bologna, Italy, March 2001.
[27] G. X. Ding, J. E. Cygler, and C. B. Kwok, ''Clinical reference dosimetry: Comparison between AAPM TG-21 and TG-51 protocols,'' Med. Phys. **27**, 1217–1225 (2000).
[28] M. S. Huq, P. Andreo, and H. Song, ''Comparison of the IAEA TRS-398 and AAPM TG-51 absorbed dose to water protocols in the dosimetry of high-energy photon and electron beams,'' Phys. Med. Biol. **46**, 2985–3006 (2001).
[29] F. Araki and H. D. Kubo, ''Comparison of high-energy photon and electron dosimetry for various dosimetry protocols,'' Med. Phys. **29**, 857–868 (2002).
[30] H. Palmans *et al.*, ''Absorbed dose to water based dosimetry vs air kerma based dosimetry for high-energy photon beams: an experimental study,'' Phys. Med. Biol. **47**, 421–440 (2002).
[31] F. M. Khan, ''Comment on 'AAPM's TG-51 protocol for clinical reference dosimetry of high-energy photon and electron beams'' [Med. Phys. **26**, 1847–1870 (1999)] Med. Phys. **27**, 445–447 (2000).
[32] B. R. B. Walters and D. W. O. Rogers, ''Monte Carlo estimates of $\%\mathrm{dd}(10)_x$ for the NPL photon beams,'' NRC Report No. PIRS-659, NRC, Ottawa, 1999.
[33] K. R. Shortt, C. K. Ross, J. P. Seuntjens, F. Delaunay, A. Ostrowsky, P. Gross, and E. Leroy, ''Comparison of dosimetric standards of Canada and France for Photons at ^{60}Co and higher energies,'' Phys. Med. Biol. **46**, 2119–2142 (2001).
[34] J. A. Purdy, W. Harms, W. F. Hanson, P. Kennedy, T. Kirby, A. Niroomand-Rad, and J. R. Palta, ''AAPM RTC TG-46: X-ray beam central axis depth-dose data for use in radiation therapy,'' Med. Phys. (1997 (draft approved by Radiation Therapy Committee)).
[35] D. W. O. Rogers, ''Fundamentals of dosimetry based on absorbed-dose standards,'' in *Teletherapy Physics, Present and Future*, edited by J. R. Palta and T. R. Mackie (AAPM, Washington, DC, 1996), pp. 319–356.
[36] R. L. Ford and W. R. Nelson, ''The EGS code system—Version 3,'' Stanford Linear Accelerator Center Report No. SLAC-210, 1978.
[37] D. Sheikh-Bagheri, ''Monte Carlo study of photon beams from medical linear accelerators; optimization, benchmark and spectra,'' PhD. thesis, Carleton University, Ottawa 1999.
[38] B. A. Faddegon, C. K. Ross, and D. W. O. Rogers, ''Forward directed bremsstrahlung of 10–30 MeV electrons incident on thick targets of Al and Pb,'' Med. Phys. **17**, 773–785 (1990).
[39] B. A. Faddegon, C. K. Ross, and D. W. O. Rogers, ''Angular distribution of bremsstrahlung from 15 MeV electrons incident on thick targets of Be, Al and Pb,'' Med. Phys. **18**, 727–739 (1991).
[40] H. Palmans, W. Mondelaers, and H. Thierens, ''Absorbed dose beam quality correction factors k_Q for the NE2571 chamber in a 5 MV and 10 MV photon beam,'' Phys. Med. Biol. **44**, 647–663 (1999).
[41] H. Palmans, W. Mondelaers, and H. Thierens, ''Beam quality of high-energy photon beams at the Ghent University linear accelerator,'' Phys. Med. Biol. **47**, L15–L18 (2002).